Supporting Online Material for

Role of Solvent-Host Interactions That Lead to Very Large Swelling of Hybrid Frameworks

C. Serre,* C. Mellot-Draznieks, S. Surblé, N. Audebrand, Y. Filinchuk, G. Férey

*To whom correspondence should be addressed. E-mail: serre@chimie.uvsq.fr

Published 30 March 2007, *Science* **315**, 1828 (2007)
DOI: 10.1126/science.111137975

This PDF file includes

Materials and Methods

Preparation of the samples. MIL-88B, MIL-88C and MIL-88D were obtained as reported before (*S1*). Prior to the collection of x-ray data, recrystallized carboxylic acid was first evacuated by extensive washing of the solids in dimethylformamide (MIL-88C) or pyridine (MIL-88B and D) at room temperature; each solid was then dried in air. In a second step, MIL-88B and MIL-88C samples were calcined overnight in air at 150°C to evacuate the solvent (pyridine, DMF). When returned to room temperature, a significant rehydration occurred for MIL-88B, with an approximate uptake of 15% water, whereas MIL-88C adsorbed water as only 3–4% of its weight. No treatment was applied to MIL-88D. These samples were then dispersed by stirring (i.e., 10 mg of solid for 1 ml of liquid) of MIL-88B, MIL-88C, and MIL-88D in various solvents such as water, methanol, ethanol, butanol, dimethylformamide, diethylformamide, dimethylsulfoxide, nitrobenzene, acetone, acetonitrile, pyridine, lutidine (2,6-dimethylpyridine), hexane, and toluene, for a few hours at room temperature. Glass capillaries were then filled with slurries and sealed to prevent evaporation of the solvent.

X-ray diffraction data. The *in situ* synchrotron powder diffraction experiments have been carried out at the Swiss-Norwegian Beamlines at the European Synchrotron Radiation Facility. The data were collected on the 1.0-mm quartz capillaries filled with the sample and a solvent, using MAR345 imaging plate at a sample-to-detector distance of 340 mm, $\lambda = 0.71118$ Å. The data were integrated using Fit2D program (Dr. A. Hammersley, ESRF) and a calibration measurement of a NIST LaB_6 standard sample.

Computer simulation. Computer simulations were used in order to yield structural models for the frameworks of the MIL-88A-B-C-D series of compounds, both in their contracted forms (narrow pore) and their solvated forms (open pores), and possibly initiate Rietveld refinement of the structures for selected compunds. For each MIL88-X solid (X = A, B, C, D), the starting structural models were obtained from the MIL-88A crystal structure, using our computational "ligand-replacement" strategy (*S1*). By substituting in the original MIL-88A topology the required ligand for the fumaric carboxylate, the framework models of MIL88-B (terephthalate), MIL-88C (2,6-naphthalene dicarboxylate), and MIL-88D (4,4'-biphenyl dicarboxylate) were generated that correspond to their observed as-synthesized cell parameters.

In this study, the as-synthesized forms of MIL-88X frameworks were used as initial models for modeling, MIL-88X-*as*. Starting from each of them, the dried (narrow pore) and solvated (open pores) forms were simulated using the cell parameters obtained by indexing the observed diffraction patterns. The simulations were performed on frameworks exclusively—i.e., in the absence of solvent molecules—in

order to yield starting framework models for further Rietveld refinement where solvent molecules could be located from difference Fourier maps.

The computational strategy is similar to the one we used for describing the swelling of the MIL-88A structure (*S2*). The main computational step consists of energy minimization for the hybrid frameworks in their original space group, *P*-62c, relaxing all atomic coordinates and cell parameters in a sequential fashion, *enforcing* either a contraction or an expansion of the cell, using the observed cell parameters as the targeted values. The key feature here is a use of carefully chosen external constraints along the cell axes—i.e., hydrostatic pressure—so as to enforce the elongation or the shrinkage of the crystal structure along specific cell axes during the energy minimizations. The hydrostatic pressure is therefore applied anisotropically, for example increasing it along *a* while keeping fixed along *c*, and vice versa. This pressure is chosen as positive when a shrinkage of the cell parameter is required or negative in the case of an elongation. This way, the initial models for all MIL-88X-*as* had their energy minimized sequentially, where the anisotropic hydrostatic pressure was carefully adjusted at each minimization step until the simulated cell parameters finally reached the targeted experimental values. This is the key point of these simulations, where the flexible hybrid framework of MIL-88 is enforced to adopt the targeted experimental cell parameters while keeping its network's connectivity identical. The above simulations were performed using the 'minimizer' of Cerius2 suite of software (*S3*) and the universal force field (*S4*) with periodic bound conditions. The force field is used as a simple mean to ensure that the so-minimized hybrid frameworks are realistic, i.e., kept within an acceptable range of structural features (bond distances, angles, and so on). Electrostatic interactions were not computed in this work.

Typically, in order to simulate the expected extended cell of MIL-88D-open (a_{final} = 20.04 Å), a negative hydrostatic pressure was first applied along the *a* axis when minimizing the initial model framework ($a_{initial}$ = 12.05 Å), while keeping the *c* cell parameter fixed. A second step was needed for applying the adequate positive hydrostatic pressure along the *c* axis ($c_{initial}$ = 27.50 Å), while keeping the *a* parameter fixed, in order to converge towards the smaller expected value (*c* = 22.91 Å). A similar approach was successively applied in order to simulate the crystal structures of all the extended and contracted cells of MIL-88X. All models converged relatively easily towards the targeted experimental cell parameters while maintaining the framework topology within realistic structural limits. Finally, the powder diffraction patterns of the different types of MIL-88*X* were simulated, and their consistency was checked against the experimental patterns.

Structure refinement. Structure refinements were done using the atomic coordinates from the computer simulation and the program Fullprof2k and its graphical interface Winplotr (*S5*, *S6*). Successive Fourier differences were performed using Shelxtl to locate the approximate position of the guest species (*S7*). Please note that we propose here only an approached structure of the latter solids filled with solvent. It is obvious that when using powder data with a low signal-to-background ratio, the position of the free solvent molecules, sometimes disordered at room temperature, is approximate, particularly in the case of the largest pore materials MIL-88C and MIL-88D.

Table S1 : *Crystal data and structure refinement parameters for* ***MIL-88B_methanol*** *or* $Cr_6O_2F_2[1,4\ BDC]_6.48CH_3OH$, ***MIL-88C_pyridine*** *or* $Fe_6O_2X_2[2,6\ NDC]_6.30C_5H_5N.48H_2O$ *and* ***MIL-88D_lutidine*** *or* $Cr_6O_2F_2[4,4'\ BPDC]_6.18C_7H_9N.30H_2O$

Formula	**MIL88B_Methanol**	**MIL-88C_Pyridine**	**MIL-88D_Lutidine**
Chemical formula	$Cr_6F_2O_{66}C_{96}H_{216}$	$Fe_6O_{80}C_{246}H_{264}$	$Cr_6F_2O_{64}N_{18}C_{258}H_{270}$
Solvant	Methanol	Pyridine	2,6-Lutidine
Molar weight ($g.mol^{-1}$)	2774	5250	4992
Calculated density ($g.cm^{-3}$)	1.36	1.53	1.04
Crystal system	Hexagonal	Hexagonal	Hexagonal
Space group	P 6_3/mmc (n°194)	P -6 2 c (n°190)	P -6 2 c (n°190)
a (Å)	15.626 (1)	18.753(1)	20.040(1)
c (Å)	15.960(1)	18.743(2)	22.911(2)
V ($Å^3$)	3375.0(3)	5708.2(4)	7968.7(2)
Z	1	1	1
Figures of merit	M_{15}/F_{15}=20/50	M_{14}/F_{14}=25/70	M_{20}/F_{20}=16/50
Radiation λ(Å)	0.71118	0.71118	0.71118
Temperature (K)	296	296	296
2θ range (°)	2-26.7	2-26.7	2-26.7
N. reflections	202	347	450
N. independent atoms	18	36	48
N. structural parameters	33	89	120
N. profile parameters	8	8	8
N. soft distance constraints	36	92	128
R_P	0.5	3.1	1.4
R_{Bragg}	21.7	19.3	23.7
Isotropic overall atomic displacement parameter	4.3(2)	5.1(2)	4.5(2)
Profile function	Pearson VII	Pearson VII	Pearson VII
Background	Experimental	Experimental	Experimental
N. of asymmetry parameters	2	2	2
Secondary phase	-----	Fe_2O_3	-----

References

(S1) S. Surblé, C. Serre, C. Mellot-Draznieks, F. Millange, G. Férey.

Chem. Commun, **2006**, 284.

(S2) C. Mellot-Draznieks, C. Serre, S. Surblé, N. Audebrand, G. Férey.

J. Amer. Chem. Soc. **2005**,16273.

(S3) Accelrys, San Diego, USA and Cambridge, UK.

(S4) Rappé, A. K.; Casewit, C. J.; Colwell, K. S.; Goddart-III, W. A.; Skiff, W. M.

J. Am. Chem.Soc. **1992**, *114*, 10024.

(S5) Rodriguez-Carvajal, J. *In "Collected Abstracts of Powder Diffraction Meeting", Toulouse, France* **1990**, 127.

(S6) Roisnel, T.; Rodriguez-Carvajal, J. *In "Abstracts of the 7th European Powder Diffraction Conference", Barcelona, Spain* **2000**, 71.

(S7) *SHELXL97*: University of Göttingen, Germany, 1997.

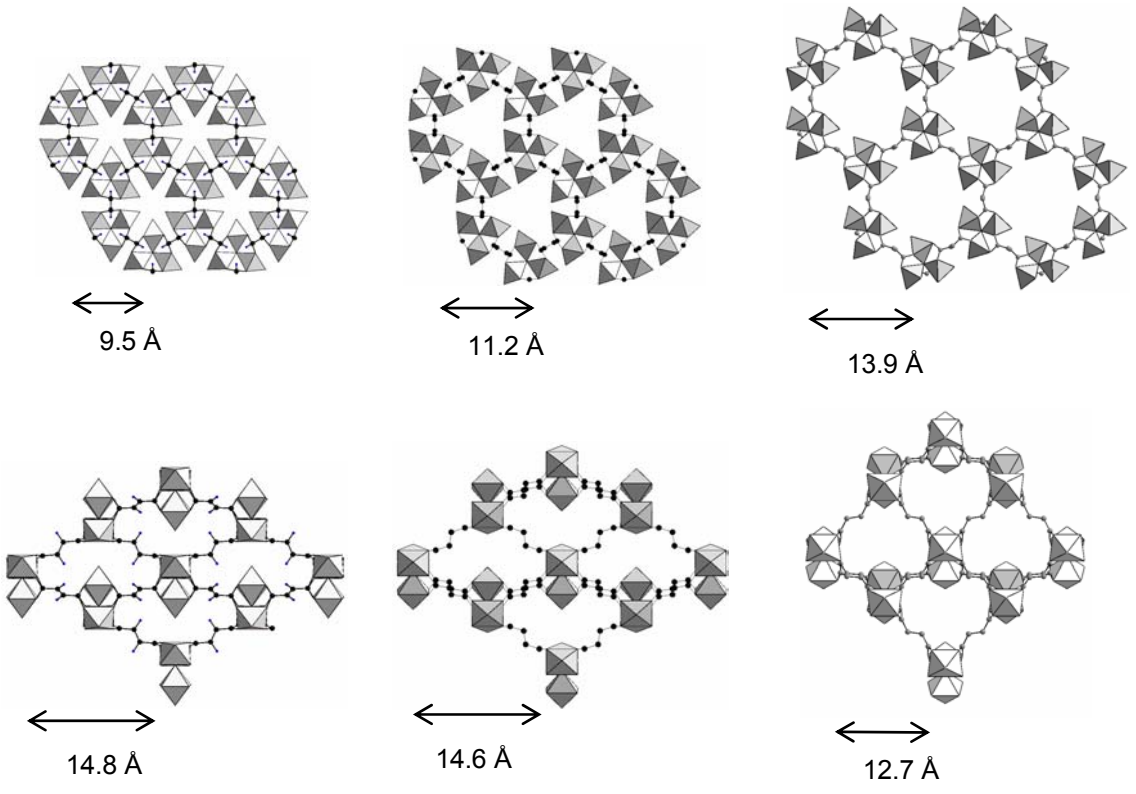

Fig. S1: view of the structure of the MIL-88A in its dry, as and open forms; top: along the c axis; bottom: along the a axis

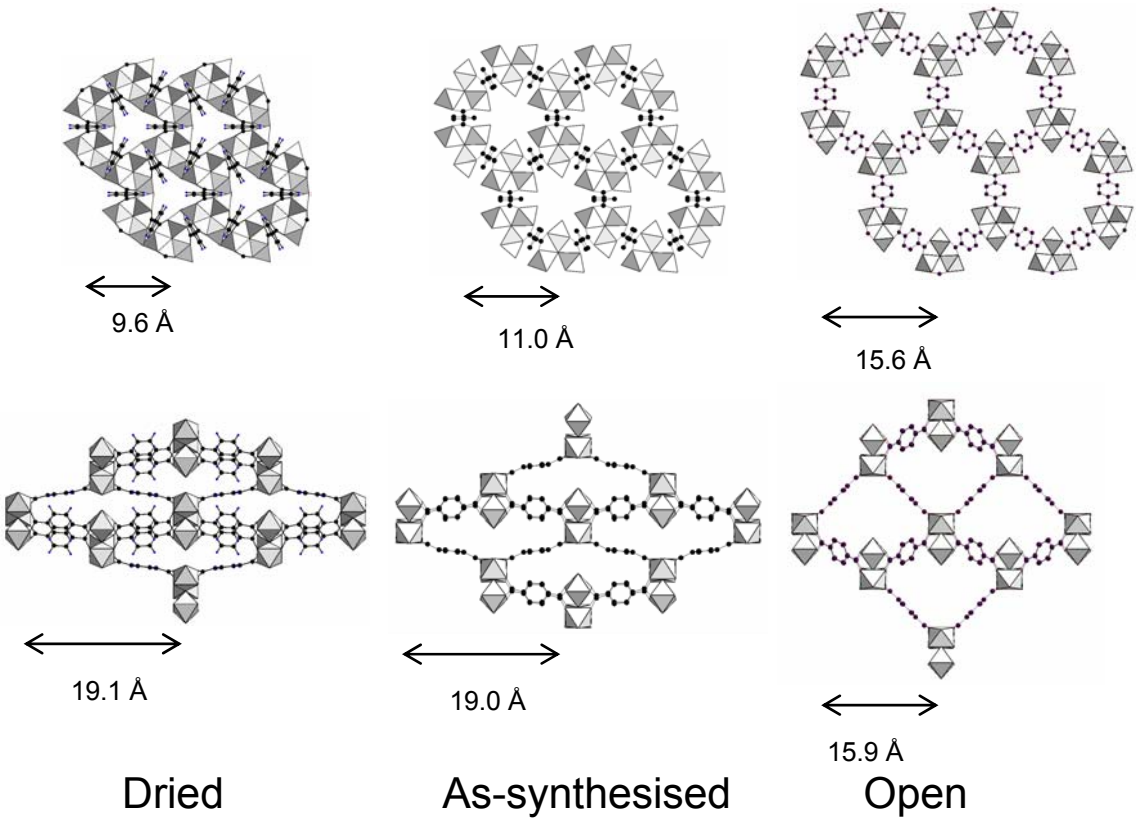

Fig. S2: view of the structure of the MIL-88B in its dry, as and open forms; top: along the c axis; bottom: along the a axis

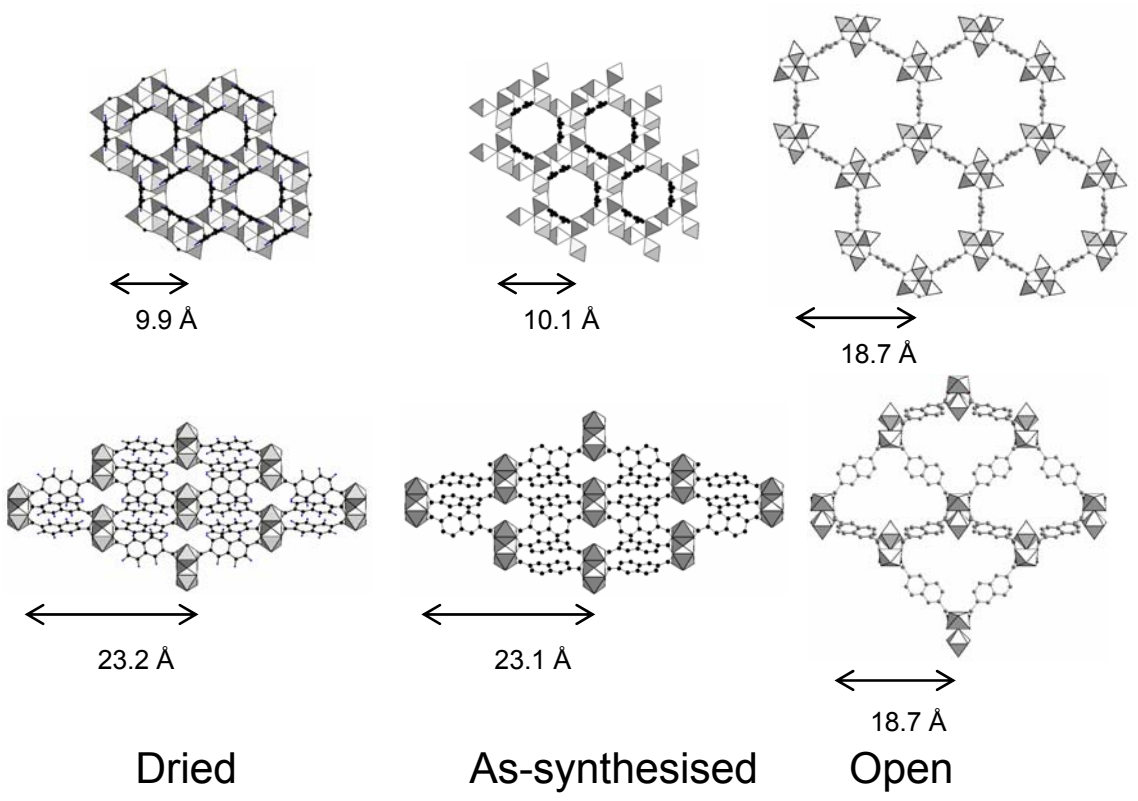

Fig. S3: view of the structure of the MIL-88C in its dry, as and open forms; top: along the c axis; bottom: along the a axis

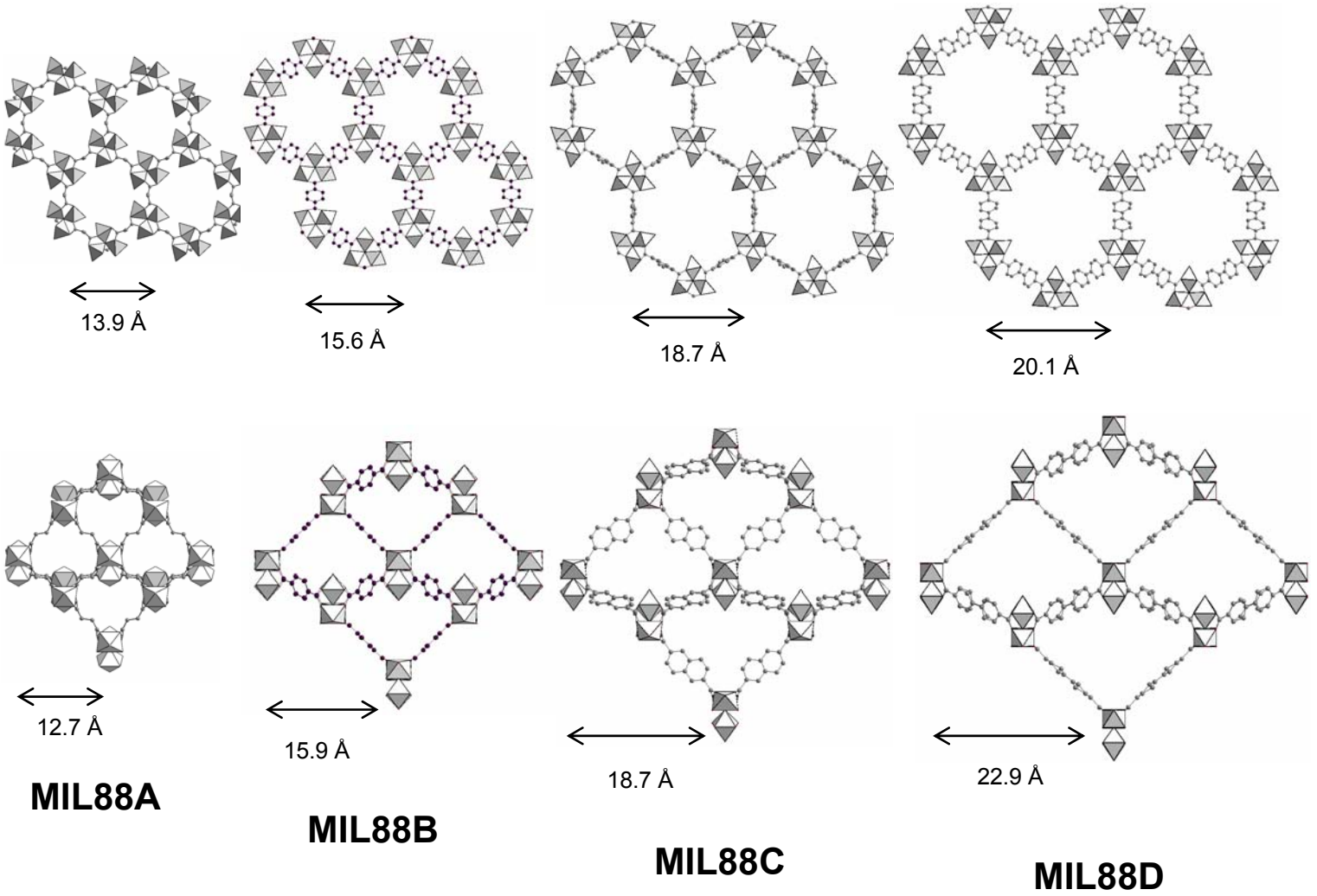

Fig. S4: view of the structure of the open forms of MIL-88A, B, C, D; top: along the c axis; bottom: along the a axis

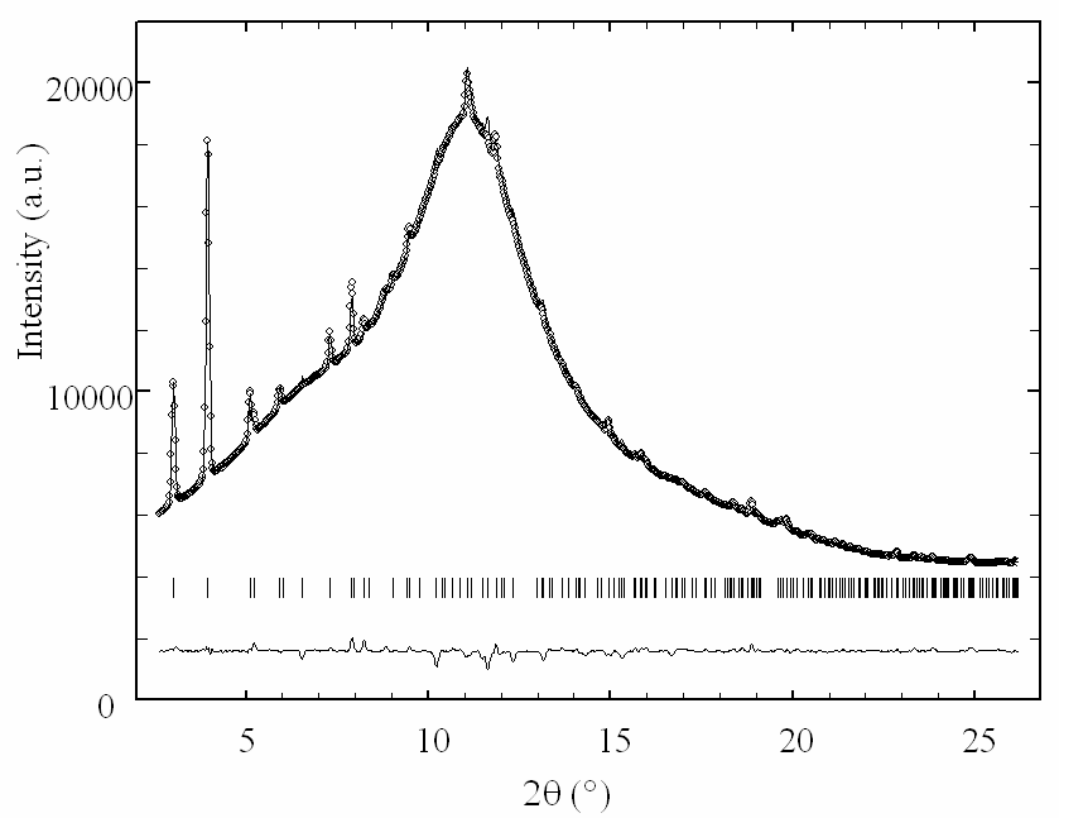

Fig. S5: Rietveld plot of MIL88B_methanol
(NB: the large hump at 2-theta=12° is due to the adsorption of methanol)

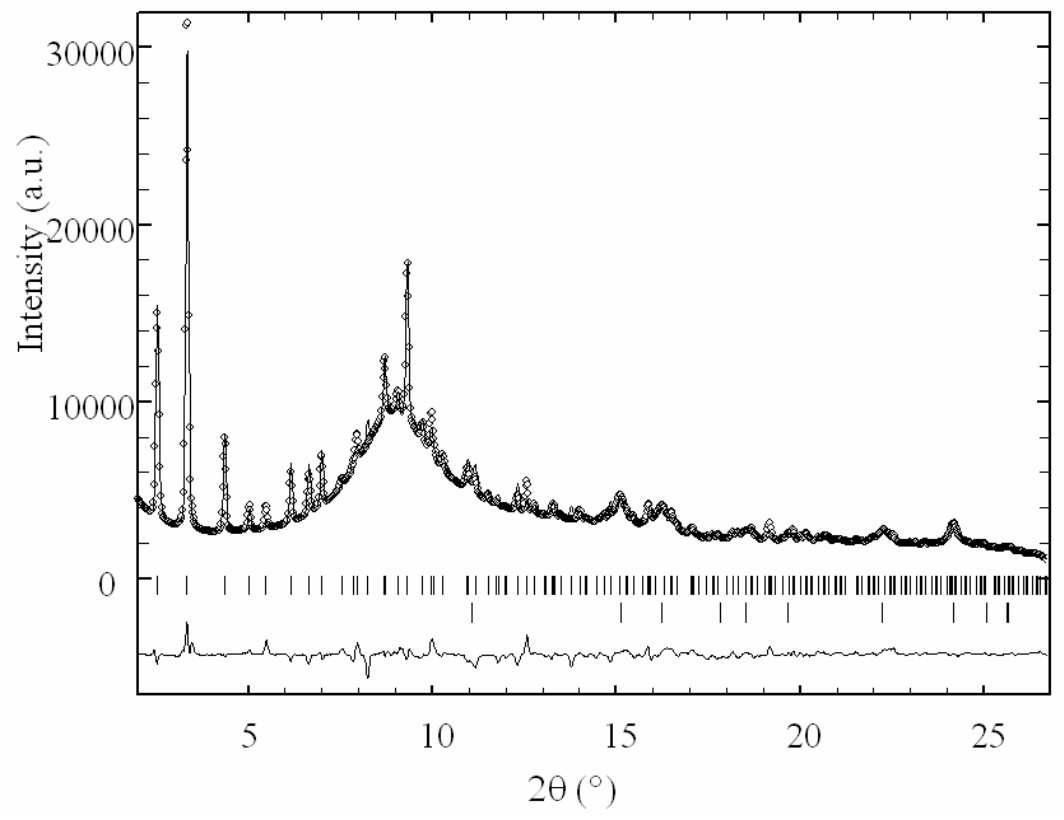

Fig. S6: Rietveld plot of MIL88C_pyridine
(NB: the large hump at 2-theta=9° is due to the adsorption of pyridine)

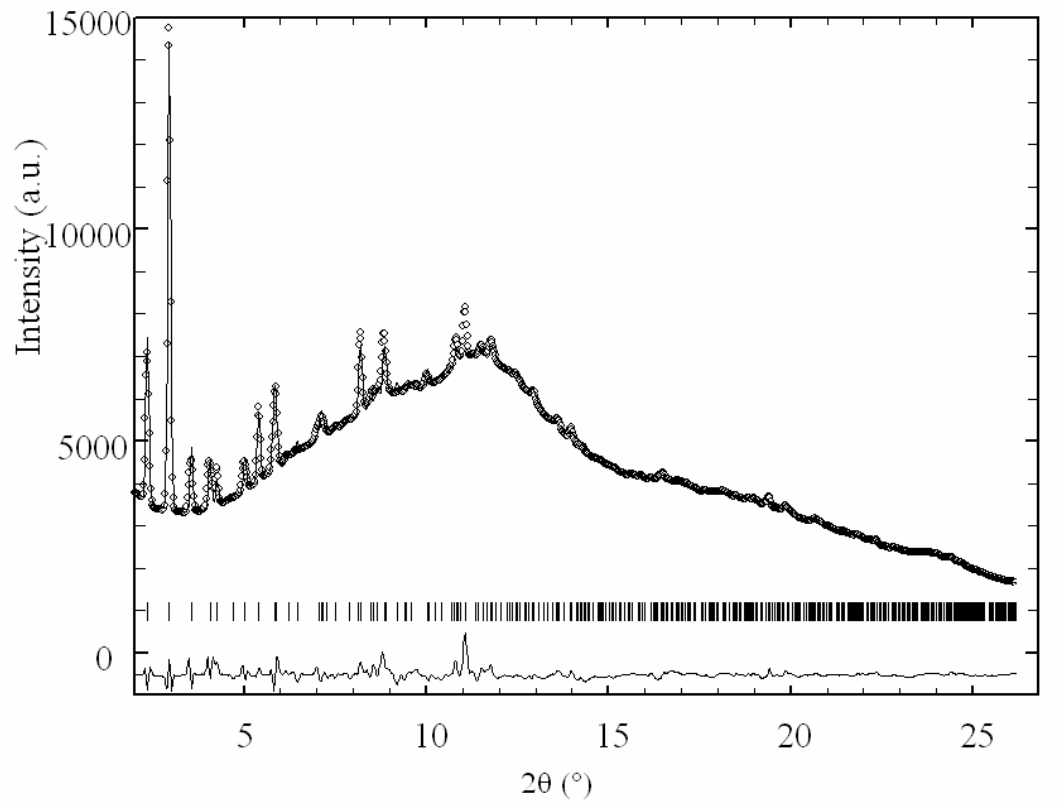

Fig. S7: Rietveld plot of MIL88D_lutidine
(NB: the large hump at 2-theta=12° is due to the adsorption of lutidine)

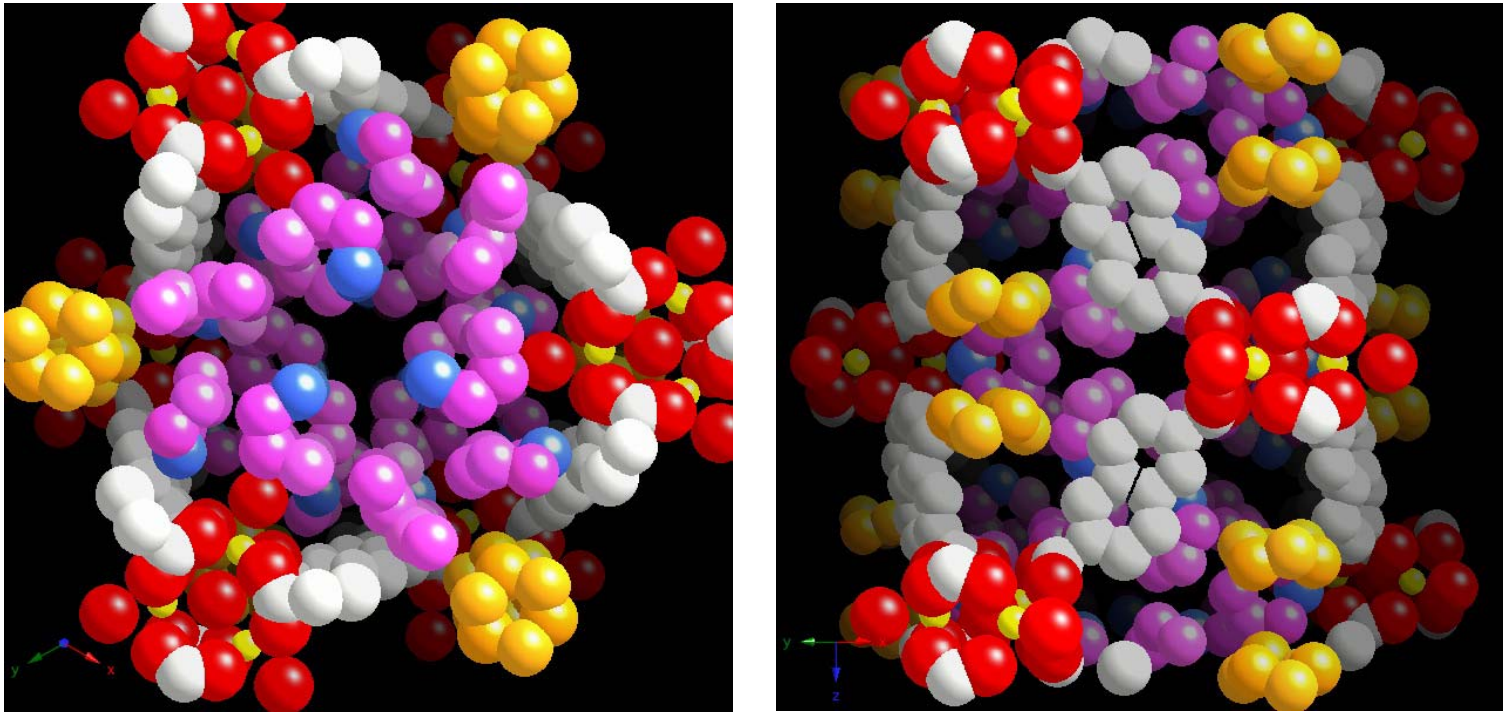

Fig. S8: Left : view of the tunnels of MIL-88C filled with pyridine; right: along the a axis
Inorganic section (yellow and red), spacer (white) and pyridine (blue, purple).

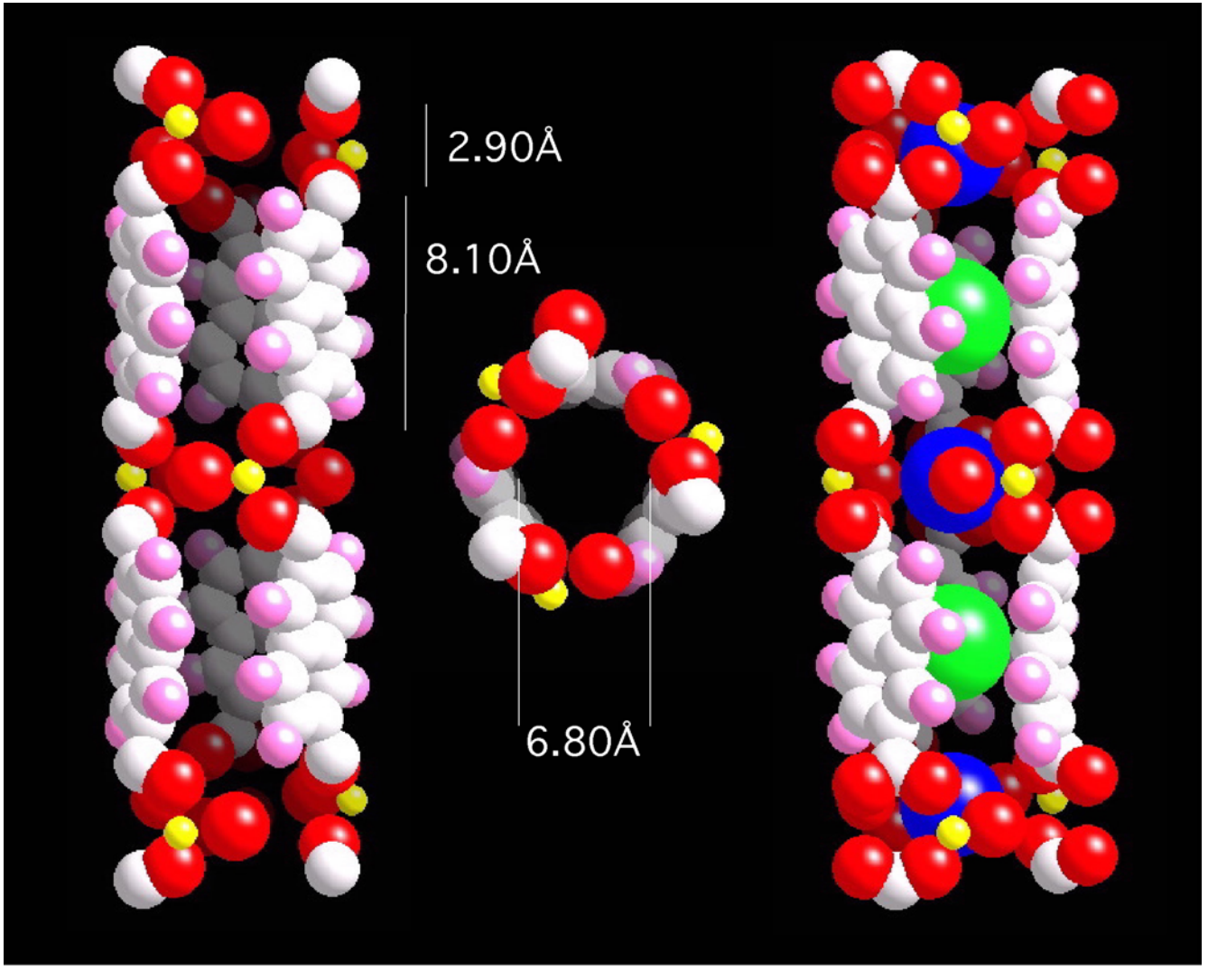

Fig. S9: Perspective view of the tunnels of MIL-88C; center: section of the tunnel; right: the tunnel with dummy atoms corresponding to the free aperture of the Inorganic section (blue) and organic one (green)

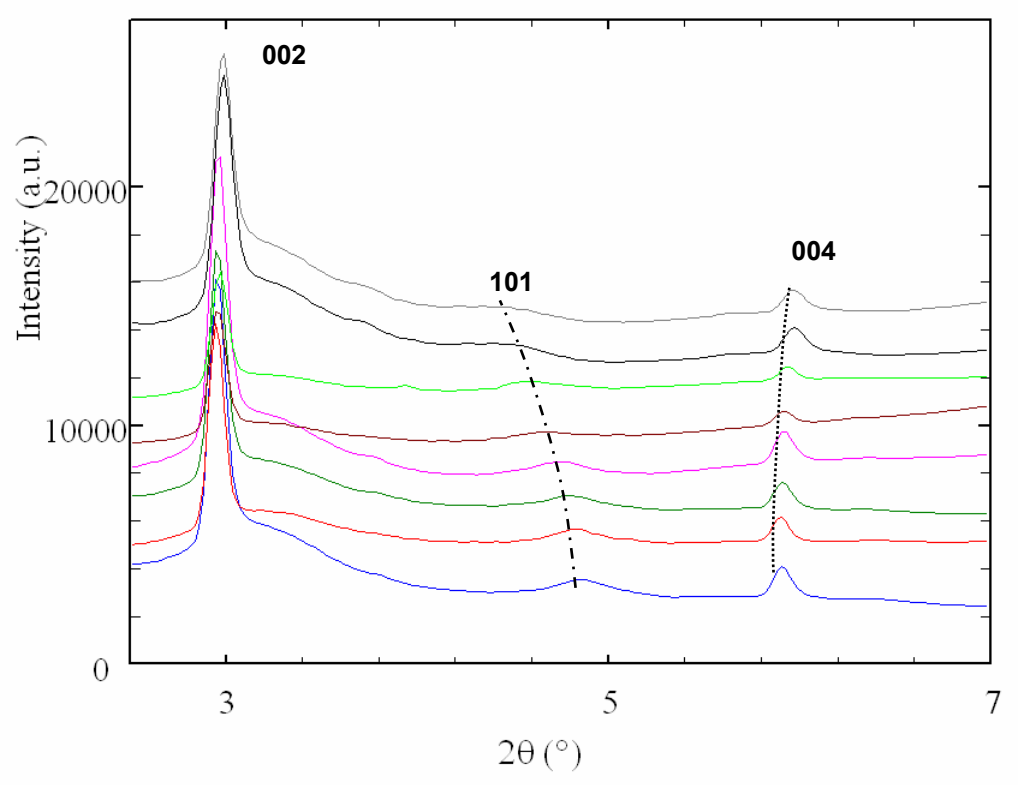

SG P-62c (n°190)

Solvant	**V(Å^3)**	**ΔV/Vdried**
Pyridine	2990	20 %
DMF	2965	19 %
MeOH, BuOH, DMSO	2800	12-13 %
Hexane, acetone, DMC, EtOH	2685	7-8 %
Lutidine, DEF	2585	3-4 %
H_2O	2535	2 %
Toluene	2500	<1 %
Dried	2490	----

Fig. S10: adsorption of liquids in MIL-88Ddry

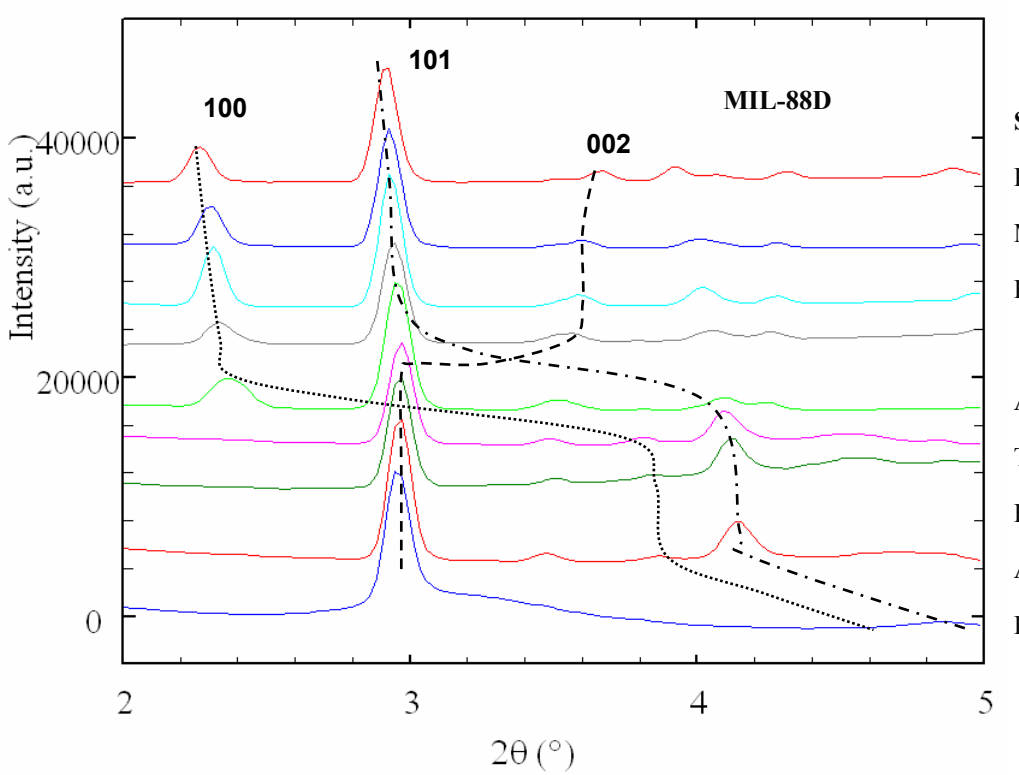

SG P-62c (n°190)

Solvant	V(Å^3)	ΔV/Vdried
Pyridine	8240	236 %
MeOH, DMC	8120	227 %
BuOH, CH_3CN	8040	226 %
DEF, Lutidine	8020	222 %
Acetone	7900	219 %
Toluene	3620	46 %
Hexane	3565	44 %
As-synthesised	3500	42 %
Dried	2480	----

Fig. S11: adsorption of liquids in MIL-88Das

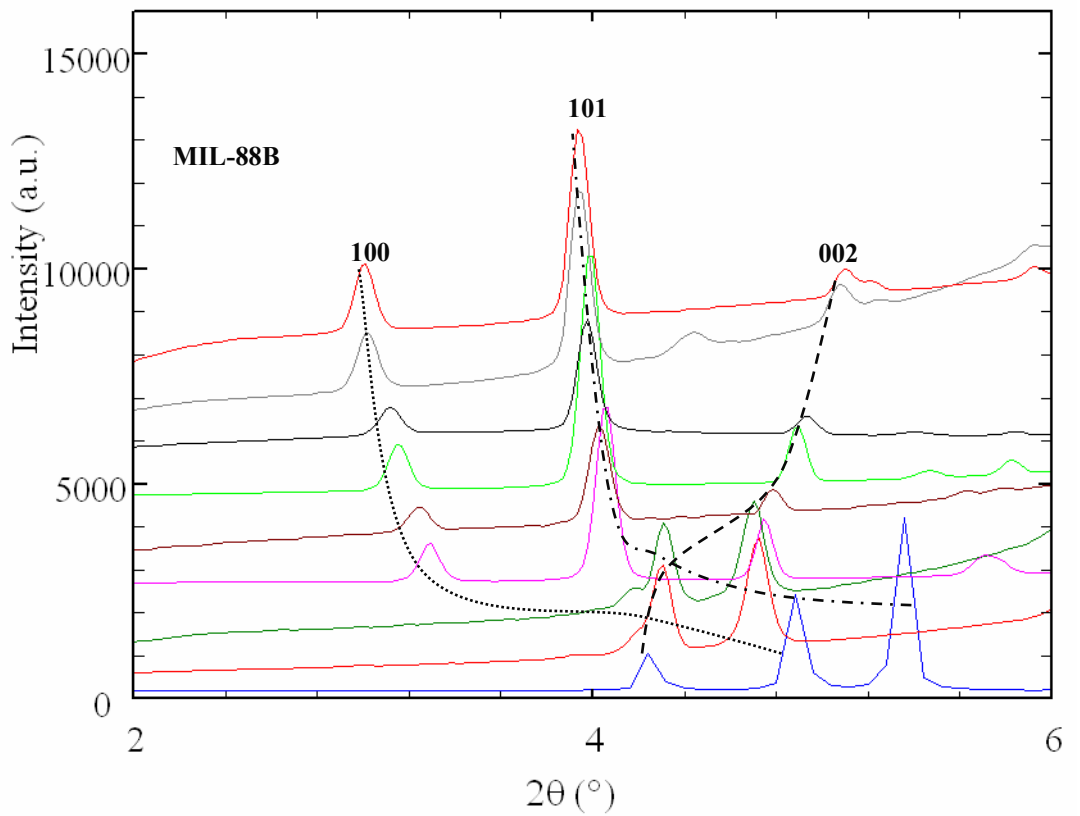

SG $P6_3/mmc$ (n°194)

Solvant	V(Å^3)	ΔV/Vdried
Methanol	3375	125 %
Lutidine	3360	124 %
Butanol	3255	117 %
DEF	3195	113 %
DMF	3095	106 %
DMSO	3025	102 %
Toluene	2085	39 %
Hexane	2055	37 %
Dried	1500	----

Fig. S12: adsorption of liquids in MIL-88Bas

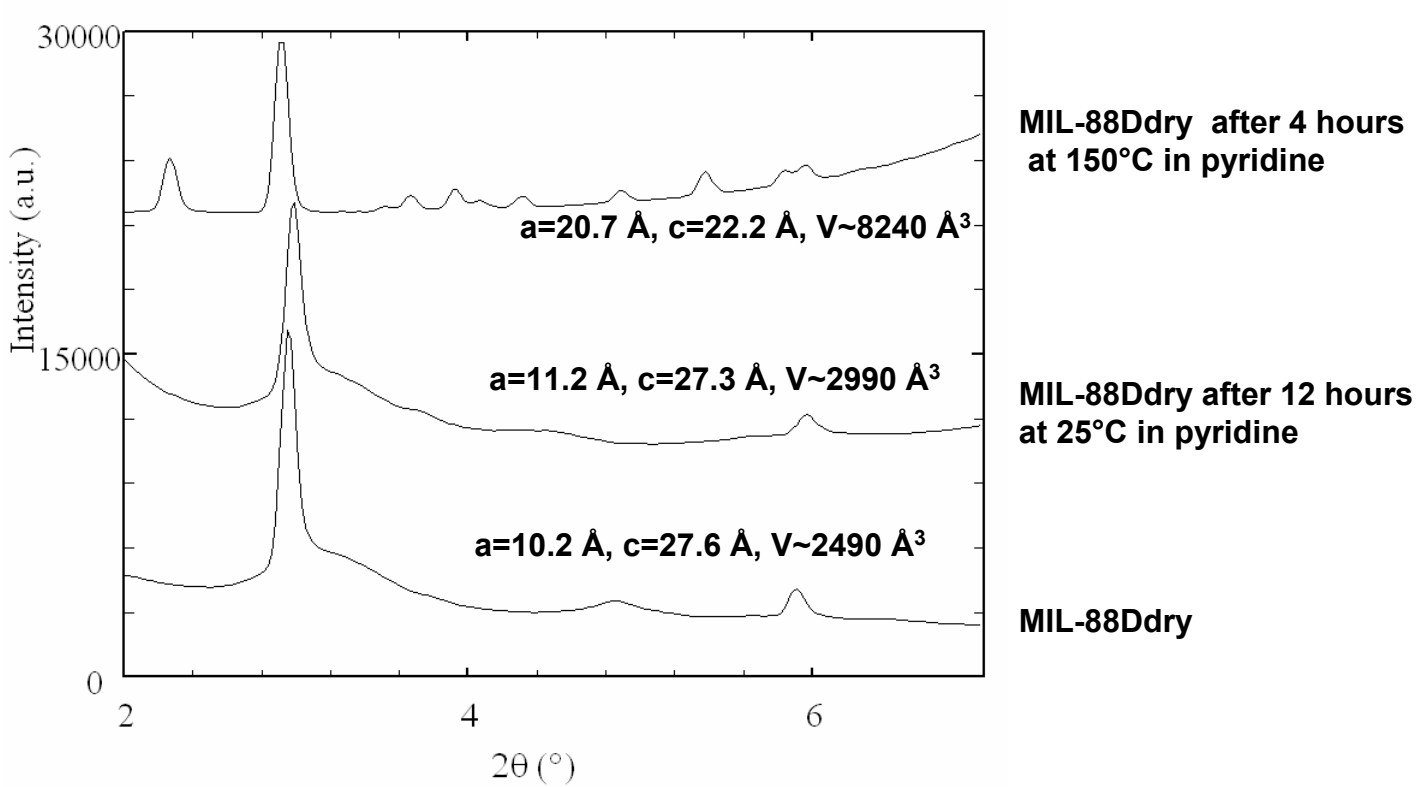

Fig. S13: effect on temperature on pyridine adsorption in MIL-88D

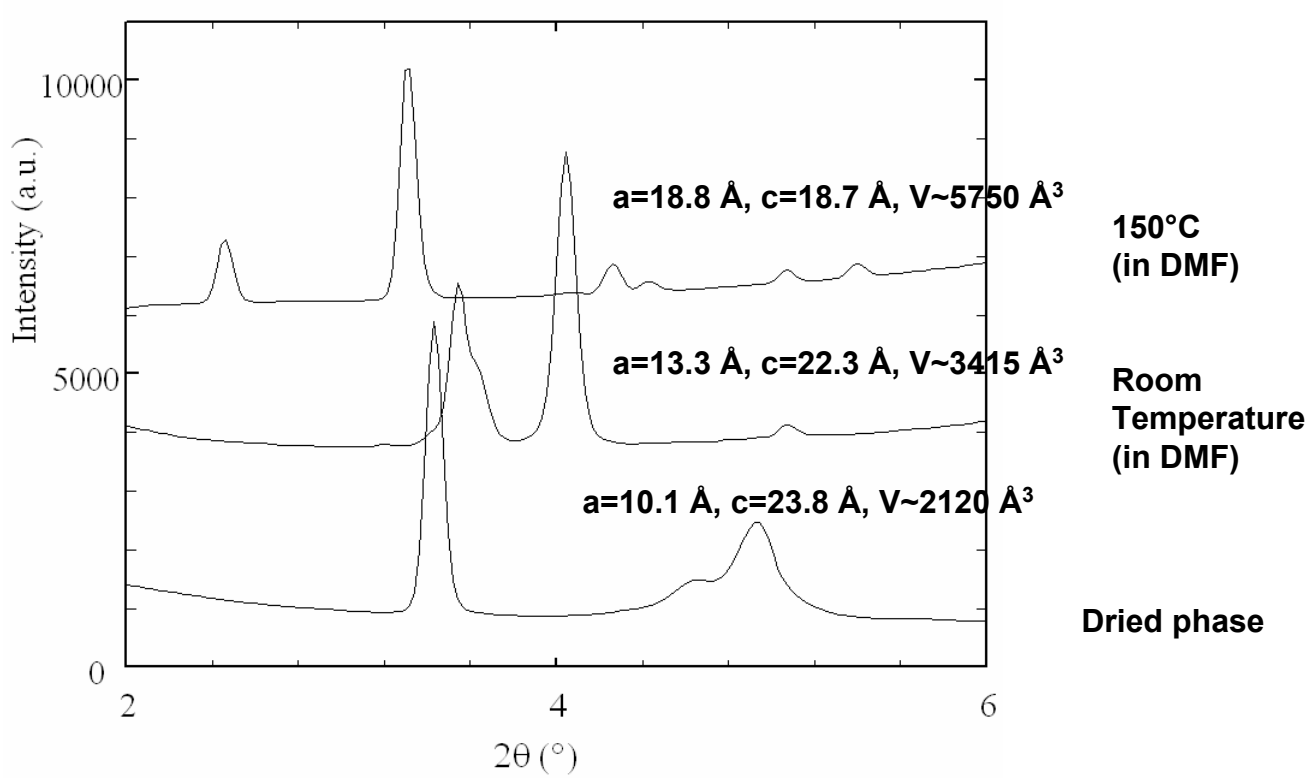

Fig. S14: effect on temperature on DMF adsorption in MIL-88C

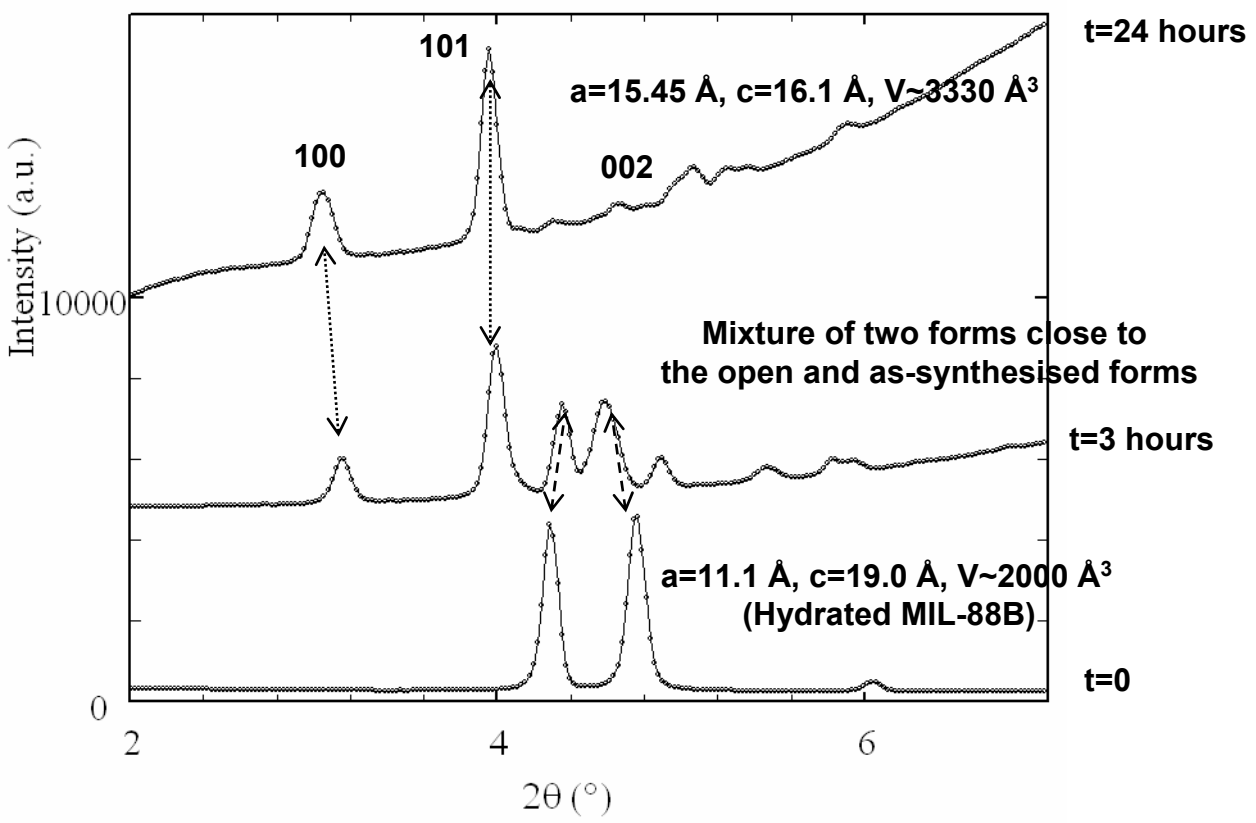

Fig.S15: X-Ray powder pattern of MIL-88B dispersed in nitrobenzene, evidencing the slow kinetics of nitrobenzene adsorption

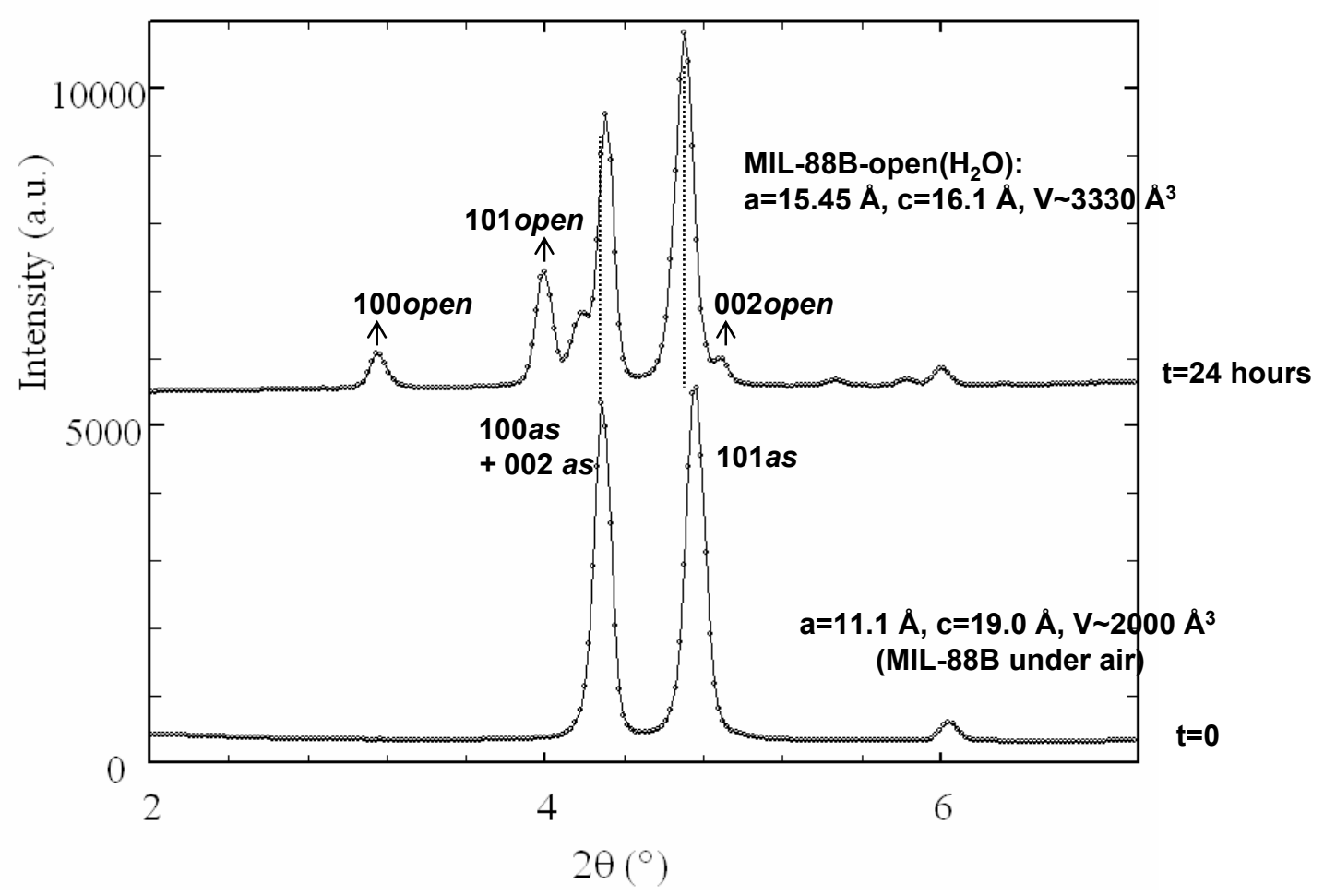

Fig.S16: X-Ray powder pattern of MIL-88B dispersed in water, evidencing the very slow kinetics of water adsorption

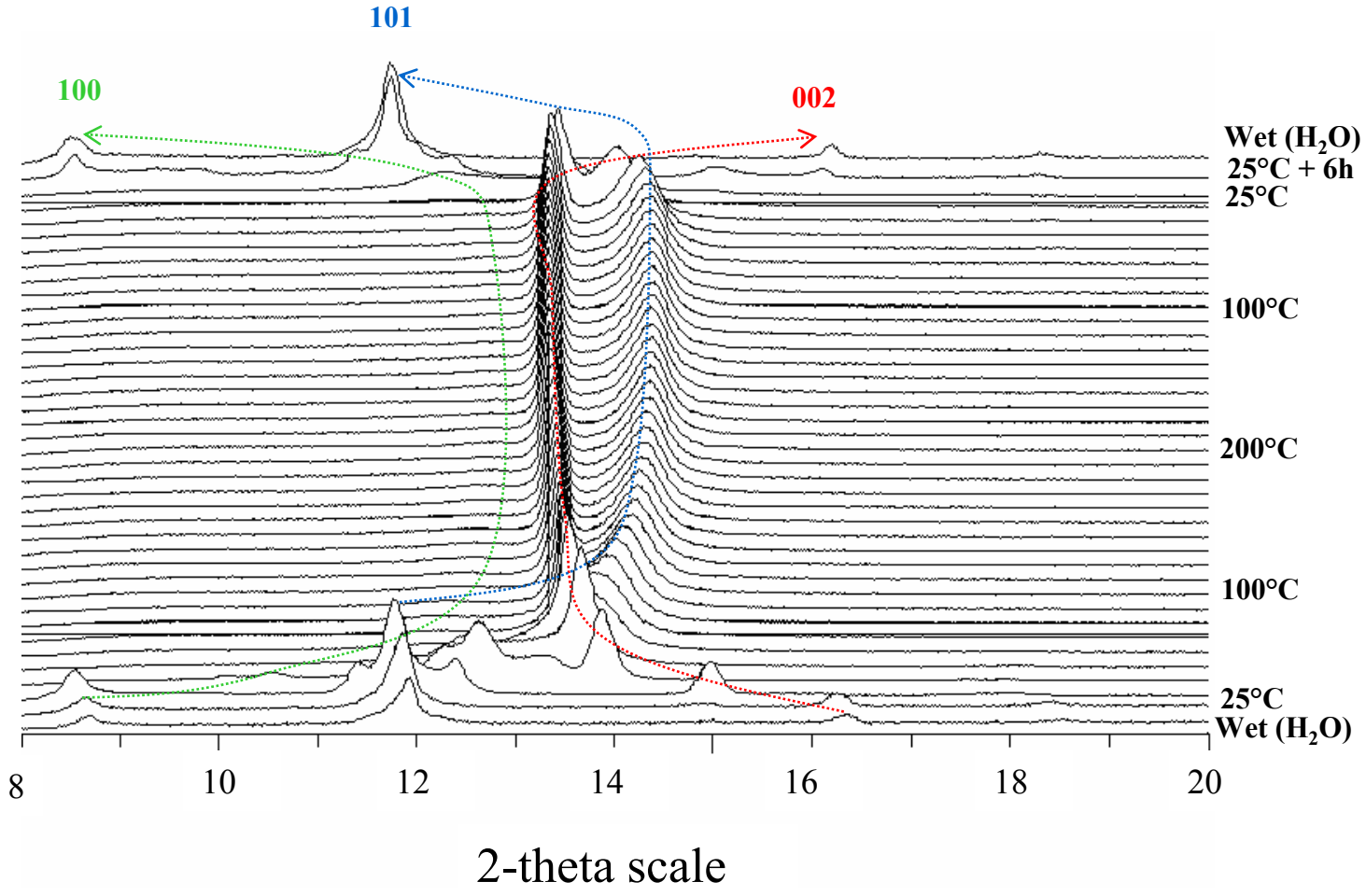

Fig.S17: X-Ray thermodiffractometry of MIL-88A under air (λ~1.79 Å)

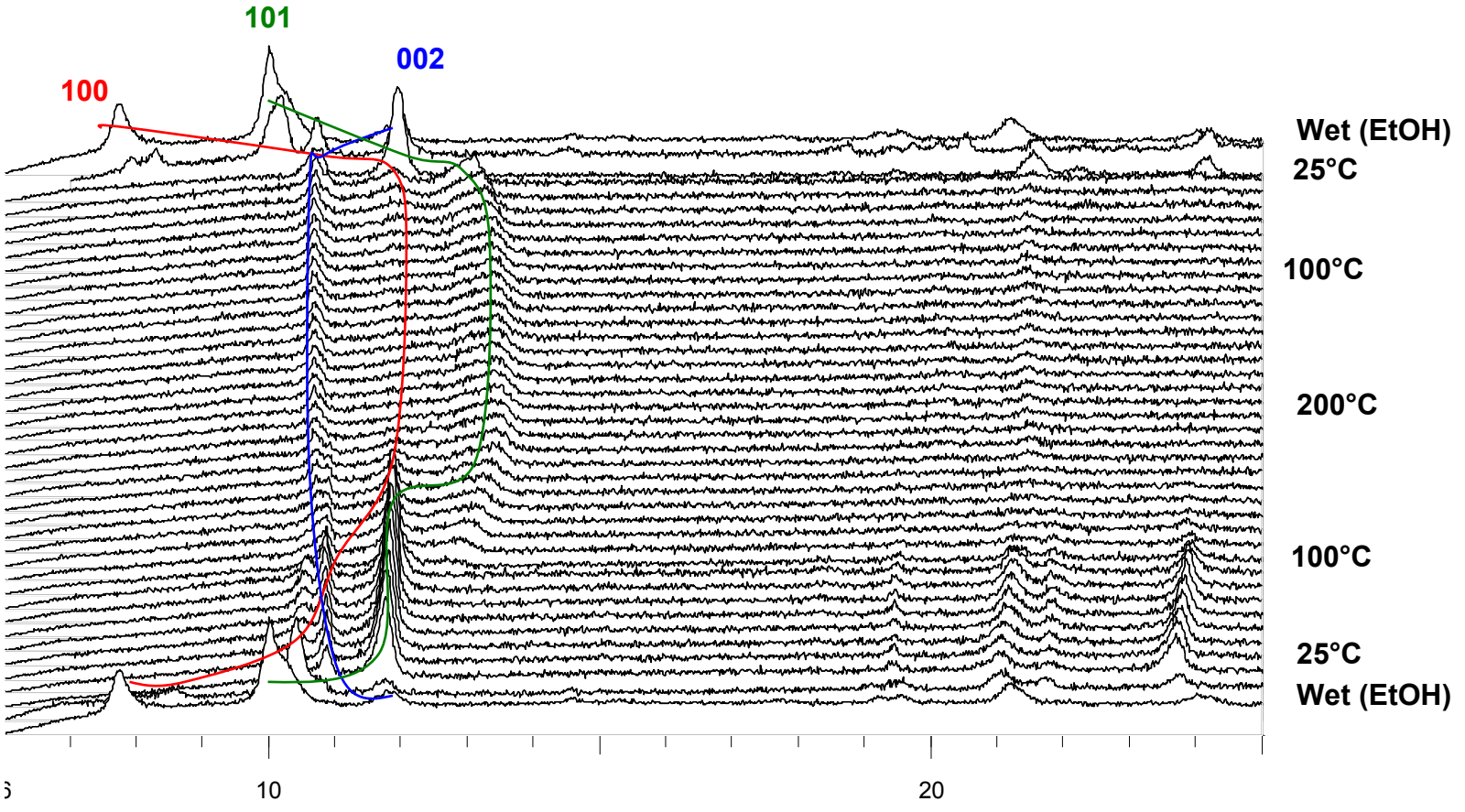

Fig.S18: X-Ray thermodiffractometry of MIL-88B under air (λ~1.79 Å)

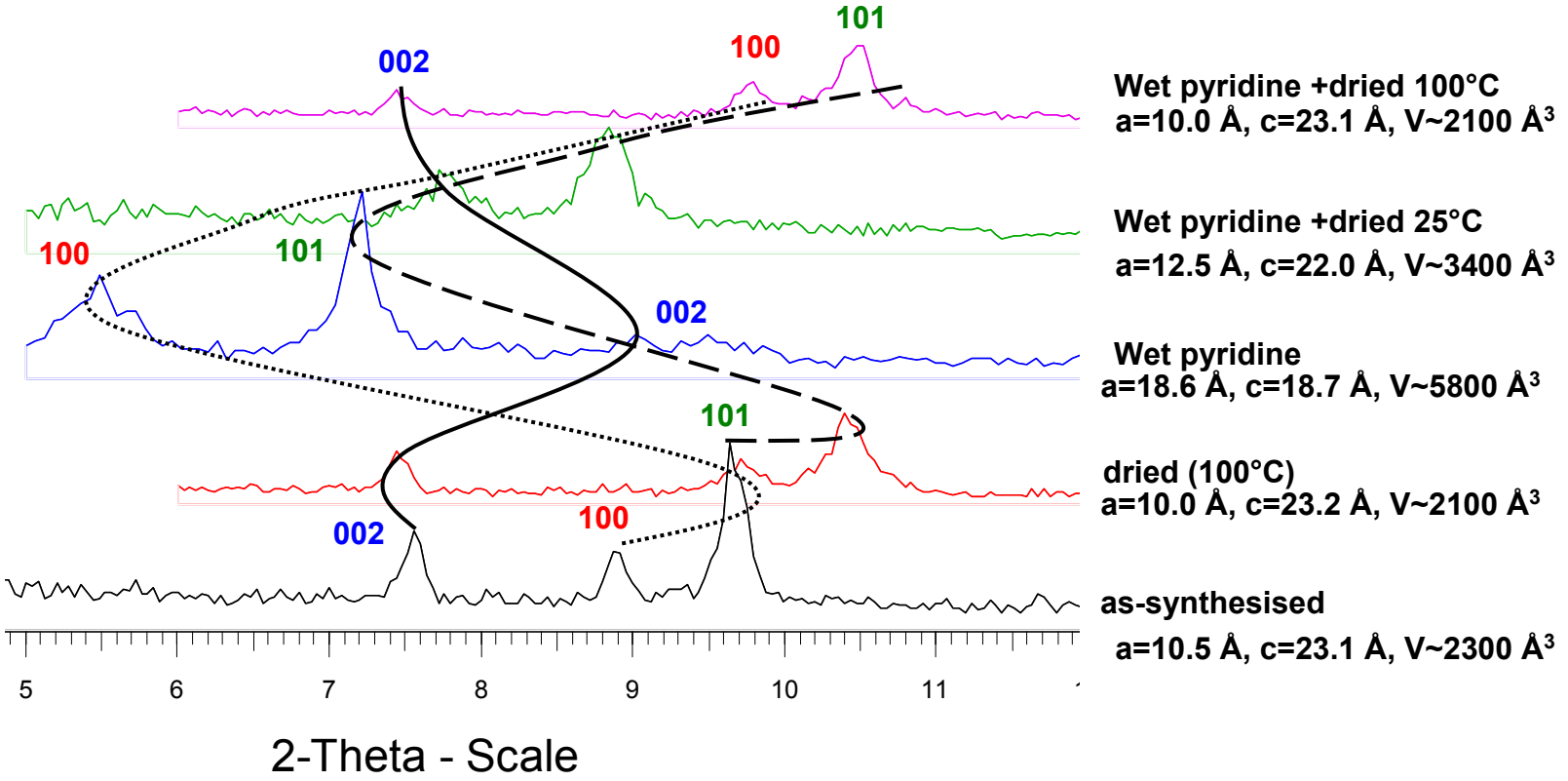

Exp. conditions : a few mg of MIL-88C has been dispersed on a glass sample holder
« Wet pyridine » means that one drop of pyridine has been dispersed on the solid

Fig.S19: X-Ray diffraction patterns of MIL-88C (powder)
under various conditions (λ~1.54 Å)

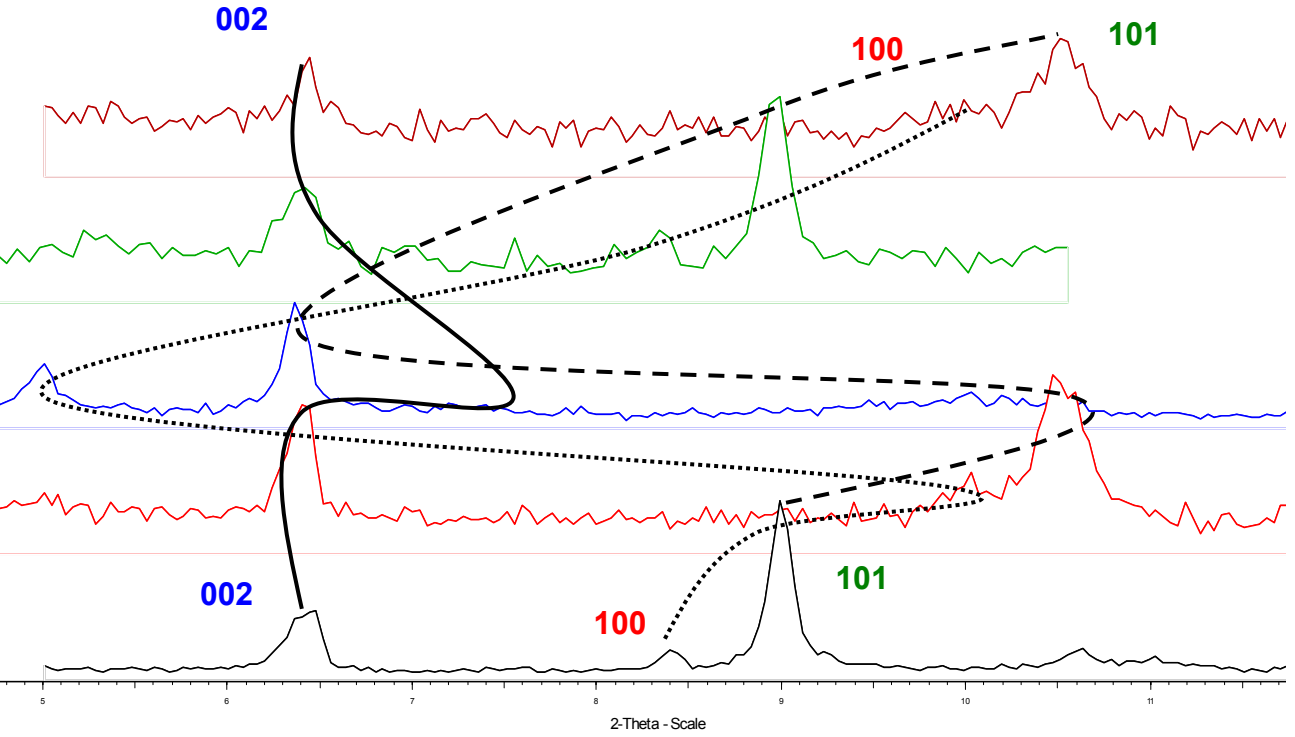

Wet pyridine +dried 100°C
a=10.0 Å, c=27.8 Å, V~2500 Å^3

Wet pyridine +dried 25°C
a=10.5 Å, c=27.6 Å, V~2800 Å^3

Wet pyridine
a=20.6 Å, c=22.1 Å, V~8200 Å^3

Dried (100°C)
a=10.0 Å, c=27.8 Å, V~2500 Å^3

As-synthesised
a=12.0 Å, c=22.0 Å, V~3500 Å^3

Exp. conditions : a few mg of MIL-88D has been dispersed on a glass sample holder
« Wet pyridine » means that one drop of pyridine has been dispersed on the solid

Fig.S20: X-Ray diffraction patterns of MIL-88D (powder)
under various conditions (λ~1.54 Å)